Catalysis Today 158 (2010) 209–214

Contents lists available at ScienceDirect

Catalysis Today

journal homepage: www.elsevier.com/locate/cattod

Photodegradation of acetone by visible light-responsive $V_2O_5/EuVO_4$ composite

Yiming He [a,*], Ying Wu [c], Tianlu Sheng [b], Xintao Wu [b,**]

[a] Department of Materials Physics, College of Mathematics, Physics and Information Engineering, Zhejiang Normal University, Yingbin Road 688, Jinhua, 321004, China
[b] State Key Laboratory of Structural Chemistry, Fujian Institute of Research on the Structure of Matter, Chinese Academy of Sciences, Fuzhou, 350002, China
[c] Institute of Physical Chemistry, Zhejiang Key Laboratory for Reactive Chemistry on Solid Surfaces, Zhejiang Normal University, Jinhua, 321004, China

ARTICLE INFO

Article history:
Available online 8 April 2010

Keywords:
Photodegradation
Photocatalyst
V_2O_5
$EuVO_4$

ABSTRACT

This paper presents a new visible-light driven photocatalyst, $VEuO_x$ composite, which was synthesized from the aqueous solutions of $Eu(NO_3)_3$ and NH_4VO_3. The photocatalyst shows high activity for photodegradation of acetone under both UV and visible light. The optimal V to Eu molar ratio is 1.5. By loading a small amount of Pt the catalytic performance of $V_{1.5}Eu_1O_x$ catalyst could be improved further. 99.4% of acetone was completely photodegradated to CO_2 and H_2O under visible light. The physical and photophysical properties of the $VEuO_x$ composite catalysts were characterized by BET, XRD, Raman, FT-IR, UV–vis spectra, and photoluminescence spectra, respectively. On the basis of the investigation results and calculated energy band positions, the origin of the high photocatalytic activity is discussed.

1. Introduction

Since Fujishima and Honda reported photo-induced decomposition of water on TiO_2 electrodes [1], a great deal of efforts have been devoted to the investigations of metal oxide semiconductor catalysts for environmental applications, such as air and water purification [2,3]. In terms of the high activity and chemical stability, TiO_2 is an excellent photocatalyst that can remove a large range of organic pollutants [4]. However, the band gap of TiO_2 (anatase, 3.2 eV) limits its absorption to the ultraviolet region (<4%) of the solar spectrum. Hence, in order to make use of solar light source in photodegradation reaction, a visible light active photocatalyst is desired.

Currently, there are two strategies to develop the visible-light driven photocatalysts: modification of TiO_2 [5–8] and exploitation of novel semiconductor materials [9,10]. Many investigations have been undertaken on the latter strategy. A great number of novel undoped single-phase mixed oxide semiconductor photocatalysts have been developed, such as $CaBi_2O_4$ [9], $BiVO_4$ [11,12], $BaBi_2Mo_4O_{16}$ [13], and $PbBi_2Nb_2O_9$ [14]. They all show a certain absorption in the visible light range. In general, these catalysts are synthesized by the conventional solid-state reactions between the corresponding oxides at high temperatures. So, one characteristic of these photocatalysts is their micro- or submicro-dimension. The larger sizes as compared to TiO_2 nanoparticles lead to higher density, thus they show good precipitation performance and can easily be recovered in water purification. Yet they have some disadvantages such as small specific surface areas, long migration distances for excited electron–hole pairs, and increasing energy-wasteful recombination; all of these were expected to lower photocatalytic activities. In order to obtain satisfied activity, these catalysts are usually loaded with a small amount of noble metals or metal oxide [15–20]. For example, Kohtani et al. [19,20] reported that the Ag-loaded $BiVO_4$ showed better activities than pure $BiVO_4$ in photo-oxidation of polycyclic aromatic hydrocarbons and 4-n-alkylphenols under visible light irradiation. Long et al. [17] found that doping of Co_3O_4 into $BiVO_4$ promoted the photocatalytic efficiency in phenole degradation reaction. Domen et al. [18] showed that RuO_2 was an effective cocatalyst that enhances the activity of $(Ga_{1-x}Zn_x)(N_{1-x}O_x)$ for overall water splitting under visible light irradiation.

In this paper, we present a new visible-light driven catalyst $V_2O_5/EuVO_4$, which shows high photocatalytic activity on photodegradation of organic substrates under visible light irradiation. $EuVO_4$ is the main phase in the photocatalyst. It has been reported that $EuVO_4$ is an important rare earth vanadate with interesting properties (such as the thermal catalytic property and the photoluminescence property) [21–24]. To the best of our knowledge, however, no studies have been focused on the photocatalytic property of $EuVO_4$. The semiconductor V_2O_5 was chosen as cocatalyst. It has been reported that loading a small amount of V_2O_5 greatly improves the photocatalytic efficiency of vanadate photocatalyst [25–27].

2. Experimental

2.1. Catalysts preparation

NH_4VO_3 (>99%), Eu_2O_3 (>99.99%), $H_2PtCl_6{\cdot}6H_2O$ (>99.95%) and P25 (Degussa TiO_2) as reference, were purchased commercially and

* Corresponding author. Tel.: +86 0579 82283920; fax: +86 0579 82283920.
** Corresponding author. Tel.: +86 0591 83714946; fax: +86 0591 83714946.
E-mail addresses: hym@zjnu.cn (Y. He), wxt@fjirsm.ac.cn (X. Wu).

0920-5861/$ – see front matter © 2010 Elsevier B.V. All rights reserved.
doi:10.1016/j.cattod.2010.03.021

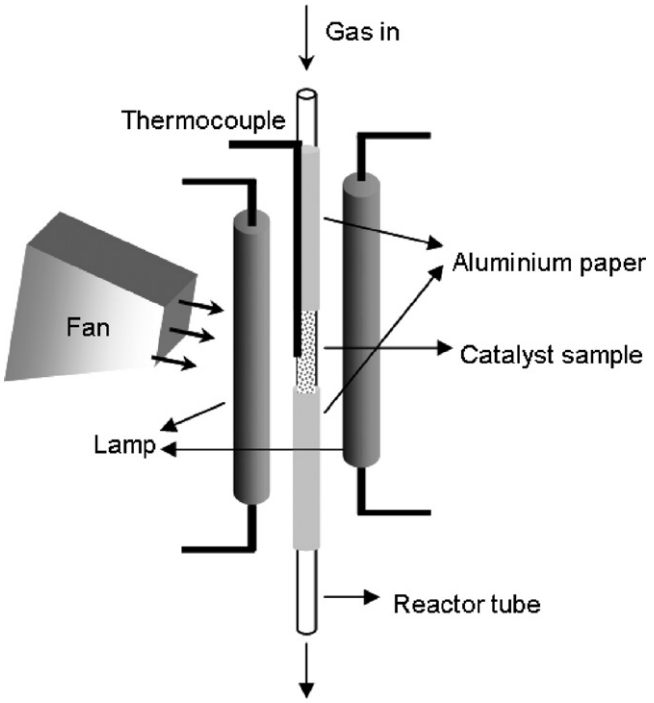

Fig. 1. The reactor system.

used without further purification. V_2O_5 was obtained by calcining NH_4VO_3 at 500 °C for 4 h. Pure $EuVO_4$ was prepared by precipitation method: solutions of NH_4VO_3 and $Eu(NO_3)_3$ (obtained by dissolving of Eu_2O_3 in HNO_3 solution) with a V to Eu molar ratio of 1.0 were mixed to obtain a deposit. The pH value of the solution was adjusted to 7–8 by a solution of NH_3. After aging at room temperature for 5 h, the deposit was filtered, washed three times by water, dried at 100 °C for 12 h and calcined at 500 °C for 4 h. The $VEuO_x$ composite catalysts were prepared by the following steps: solutions of NH_4VO_3 and $Eu(NO_3)_3$ with different V/Eu molar ratios were mixed and evaporated to give a solid precursor. After dried at 100 °C for 12 h, the precursor solid was calcined at 500 °C for 4 h and then cooled to room temperature to yield the catalyst.

The 0.1 wt.% $Pt/V_{1.5}Eu_1O_x$ catalyst was prepared by impregnation-photoreduction method: 4.5 g of $V_{1.5}Eu_1O_x$ catalyst was added into 3.0 mL of $H_2PtCl_6{\cdot}6H_2O$ solution (Pt: 0.0015 g/mL). The sample was kept in the dark for 5 h, and then dried at 80 °C for 10 h. After that, the dried sample was irradiated by Hg lamp (or Xe lamp) ion for 2 h (the strong light decomposed the H_2PtCl_6 to metal Pt) to obtain the 0.1 wt.% $Pt/V_{1.5}Eu_1O_x$ catalyst.

2.2. Catalytic tests

The catalytic reaction under UV light was carried out in a quartz tube (ID 5.0 mm) reactor and two 500 W high pressure mercury lamps were used as UV light sources. When the reaction was carried out under visible light, two 400 W xenon lamps were used as visible light sources and a glass tube (ID 5.0 mm) reactor which could cut off most of the UV light was used. In either reactor, the bed length of catalyst (500–800 mg) was about 4.5 cm and the rest parts of the reactor were wrapped by aluminum paper to exclude the contribution of the blank reaction (Fig. 1). A thermocouple which clung to the reactor closely was used to detect the reaction temperature. The reactor tube was cooled by a fan. Because of the heat from the lamps, although we tried to cool down the reactor by the fan, the temperature was still between 130 and 140 °C (due to the heat of reaction, the temperature inside the reactor tube was higher. The real reaction temperature was observed to be between 140 and 170 °C). Pure oxygen was used as oxidant. The organic reactants (acetone, methanol, ethanol, 2-propanol, benzene) were fed into the reactor by bubbling gas (O_2) through liquid organic at 0 °C (cooled in a water-ice bath) to obtain the reactant mixture. The flow of the mixture was controlled at 8.0 mL/min. The concentration of organics was analyzed by GC and the results are shown in Table 2. Before each catalytic testing, the photocatalyst was allowed to equilibrate in the reaction gas for at least 60 min. The reaction products were analyzed on a GC (equipped with a GDX-203 column and a 5A carbon molecular sieve column) with TCD. All the data were collected after 3 h of online reaction.

In order to rule out the thermal reaction, both the $V_{1.5}Eu_1O_x$ and 0.1 wt.% $Pt/V_{1.5}Eu_1O_x$ catalysts were tested for acetone oxidation in the dark at the same reaction temperature (170 °C). The dark reaction shows that acetone did not react with oxygen over $V_{1.5}Eu_1O_x$ or 0.1 wt.% $Pt/V_{1.5}Eu_1O_x$ catalysts at 170 °C. The blank reaction was also tested. The result shows that no acetone was photodegradated without photocatalyst under visible light.

2.3. Characterizations

The XRD characterization of catalysts was carried out on RIGAKU DMAX2500 using Cu Kα radiation (40 kV/40 mA). The specific surface areas were measured on Autosorb-1 (Quantachrome Instruments). The Raman spectra of the catalysts were collected on RM1000 spectrometer (Renishaw) with an Ar ion laser (514.5 nm) as excitation source. The FT-IR spectra of the catalysts were recorded on PerkinElmer Magna 750 with a resolution of 4 cm^{-1}. The UV–vis spectra of catalysts were recorded on a UV–vis spectrometer (PerkinElmer Lambda900) equipped with an integrating sphere. The photoluminescence (PL) spectra of catalysts were collected on FLS-920 (Edinbergh Instrument). The light source was a Xe lamp (excitation at 280 nm).

3. Results and discussion

3.1. Characterization of the catalysts

3.1.1. BET and XRD analyses of catalysts

The BET results are shown in Table 1. Both Eu_2O_3 and V_2O_5 had low specific surface areas. The specific surface area of $EuVO_4$ was equal to 20 m^2/g. In comparison with $EuVO_4$, $V_1Eu_1O_x$ catalyst had a larger surface area, although they had the same V to Eu molar ratio. With the increase of V/Eu ratio, it is found that the BET surface area of $VEuO_x$ catalysts decreased.

Fig. 2 presents the XRD patterns of VEuO catalysts. Pure Eu_2O_3 shows several peaks at $2\theta = 19.9°$, 28.3°, 32.8°, 47.2°, and 56.0° (JCPDS 43-1008), while pure $EuVO_4$ shows several strong diffraction peaks at 18.5°, 24.5°, 33.0°, and 49.0° (JCPDS 15-0809). $V_1Eu_1O_x$ catalyst has nearly the same XRD pattern as $EuVO_4$, indicating only $EuVO_4$ phase was detected. When the V/Eu molar ratio was increased to 1.5, several peaks at $2\theta = 15.3°$, 20.3°, 26.1° corresponding to V_2O_5 phase (JCPDS 41-4126) was observed. With the increase in vanadium concentration, the peak intensity of V_2O_5 increased.

Table 1
Specific surface area of catalysts.

Catalysts	Eu_2O_3	$V_1Eu_1O_x$	$V_{1.5}Eu_1O_x$	$V_{2.5}Eu_1O_x$	$V_{3.5}Eu_1O_x$	$EuVO_4$	V_2O_5
S (m^2/g)	4	42	25	20	17	20	6

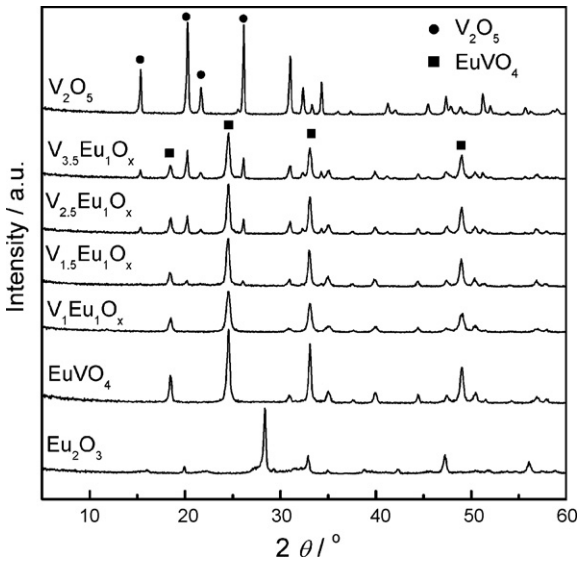

Fig. 2. XRD patterns of $VEuO_x$ composites.

Except the V_2O_5 and $EuVO_4$ phases, no new phase was found in the $VEuO_x$ composite catalysts.

3.1.2. FT-IR and Raman analysis of catalysts

Fig. 3 shows the FT-IR spectra of $VEuO_x$ composite catalysts. Eu_2O_3 shows two weak peaks at 1395 and 1362 cm^{-1}. $EuVO_4$ has a strong broad peak between 750 and 950 cm^{-1} and a shoulder peak at 946 cm^{-1}. $V_1Eu_1O_x$ catalyst had the same V/Eu molar ratio with $EuVO_4$. So, the similar FT-IR spectrum was observed. However, besides the peaks of $EuVO_4$ another weak peak at 1020 cm^{-1} was observed over $V_1Eu_1O_x$ catalyst, which could be assigned to the V=O stretching vibration in the V_2O_5 phase [28]. Obviously, there exist both $EuVO_4$ and V_2O_5 phases in $V_1Eu_1O_x$ composite. The same two phases were also detected in other $VEuO_x$ composites. With the increase of the V/Eu molar ratio, the peak of the V_2O_5 phase became stronger. The FT-IR characterizations are consistent to those of XRD shown in Fig. 3.

Both the XRD and FT-IR analysis of the $VEuO_x$ composite catalysts showed that only V_2O_5 and $EuVO_4$ phases were formed in catalysts. This result could also be proved by the Raman analysis.

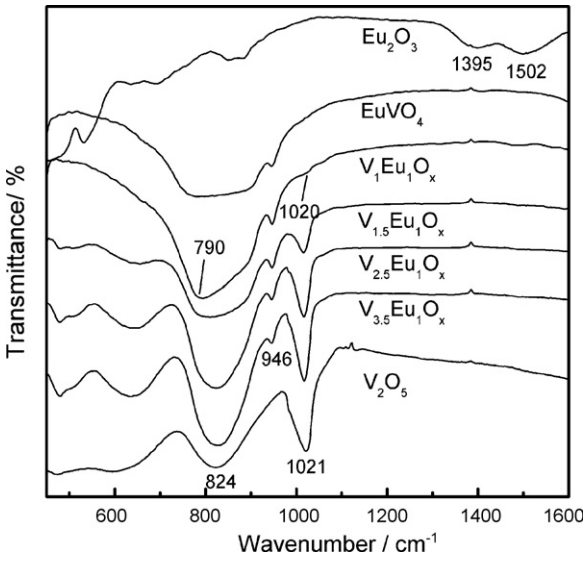

Fig. 3. FT-IR spectra $VEuO_x$ composites.

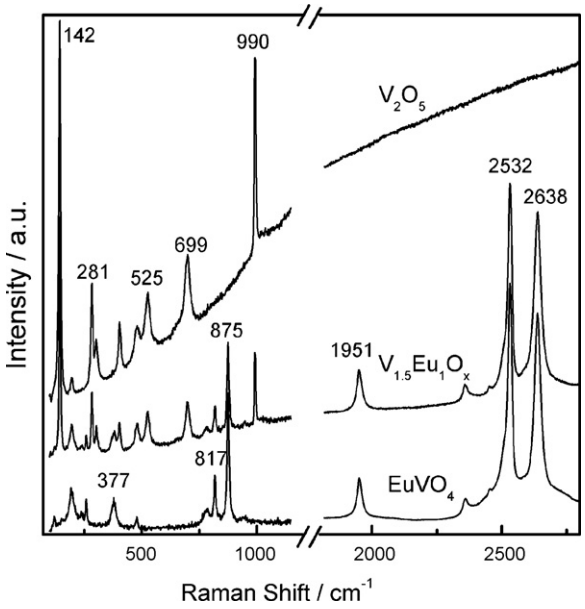

Fig. 4. Raman spectra of $VEuO_x$ composite catalysts.

Fig. 4 shows the Raman spectra of the catalysts. In order to make clarity, only V_2O_5, $V_{1.5}Eu_1O_x$, and $EuVO_4$ catalysts are presented. $EuVO_4$ has several strong peaks at 377, 817, 875, 1951, 2532, and 2638 cm^{-1}, while V_2O_5 shows several strong peaks at 142, 281, 525, 699, and 990 cm^{-1}. The Raman spectrum of $V_{1.5}Eu_1O_x$ shows that there is some V_2O_5 phase besides the $EuVO_4$ phase. No new peaks (belonging to a new phase) were observed over the surface of the catalyst.

3.1.3. UV–vis analysis of catalysts

The UV–vis spectra of P25 (TiO_2 Degussa), $EuVO_4$, V_2O_5 and $VEuO_x$ catalysts are shown in Fig. 5. Both Eu_2O_3 and P25 could only absorb the UV light ($\lambda < 400$ nm). They show the color of white. The color of pure $EuVO_4$ is pale yellow, which indicates $EuVO_4$ could absorb the visible light. As shown in Fig. 5, the band gap absorption edge of $EuVO_4$ is determined to be 554 nm, corresponding to the band gap energy 2.24 eV, which is consistent with the result of Prasad [29]. Compared with $EuVO_4$, V_2O_5 has a smaller band gap (2.08 eV) and could absorb most of the visible light. So, loading of V_2O_5 to $EuVO_4$ greatly promoted the catalyst's photoadsorption performance. Such as $V_1Eu_1O_x$ catalyst, its peak intensity in the vis-

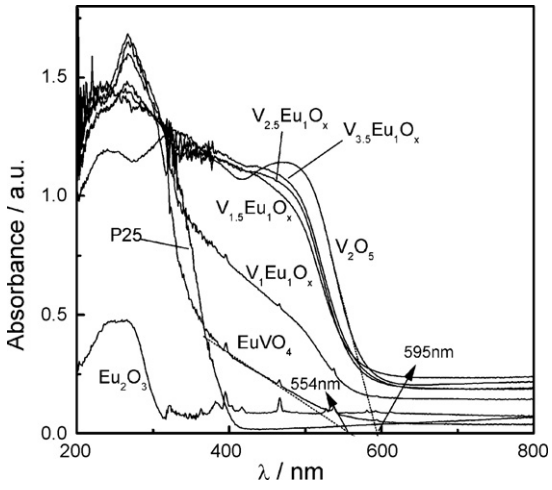

Fig. 5. UV–vis spectra of $VEuO_x$ composite catalysts.

Table 2
Photocatalytic oxidation of organics over $V_{1.5}Eu_1O_x$ and 0.1 wt.% $Pt/V_{1.5}Eu_1O_x$ catalyst in the visible region.

Organics	Methanol	Ethanol	Acetone	2-Propanol	Benzene
X (mol%)	5.0	1.5	10.0	1.0	2.2
Conv. (%)	100(100)	99.6 (100)	98.0 (99.4)	98.3 (100)	30.7 (98.9)
S_{CO_2} (%)	15.1 (100)	44.8 (100)	39.3 (100)	53.7 (100)	79.1 (100)
S_{CO} (%)	84.9 (0)	55.2 (0)	60.5 (0)	42.6 (0)	20.9 (0)
S_{others} (%)	0 (0)	0 (0)	0.2 (0)[a]	3.7 (0)[b]	0 (0)

Note: The numbers in bracket represent the performance of 0.1 wt.% $Pt/V_{1.5}Eu_1O_x$ catalyst. X is the molar concentration of organic compound in oxygen.
[a] Selectivity to acetol.
[b] Selectivity to acetone.

ible region (400–600 nm) is higher than pure $EuVO_4$, which could be due to the small amount of V_2O_5 detected by FT-IR. With the increase in vanadium content, the photoadsorption performance of $VEuO_x$ composites increased. But when the molar ratio of V to Eu was larger than 1.5, only a little difference was observed.

3.2. Photocatalytic performance of catalyst

The photocatalytic performance of catalysts was evaluated in the photodegradation reaction of acetone under UV and visible light. Fig. 6 shows the photocatalytic activities of P25 (TiO_2, Degussa), Eu_2O_3, V_2O_5, $EuVO_4$, and $VEuO_x$ composite catalysts. Under UV light, P25 had a high activity for acetone degradation. 99.1% of acetone conversion was obtained. But under visible light, P25 shows low activity like V_2O_5. Eu_2O_3 was inactive under visible light and showed weak activity for acetone degradation under UV light. Compared with V_2O_5 or Eu_2O_3, pure $EuVO_4$ shows higher activity. 56.4% of acetone conversion was obtained under UV light, and under visible light the acetone conversion reached 44.6%. However, its activity is still lower than the $VEuO_x$ composite catalysts. As shown in Fig. 6, the acetone degradation conversion increased with the increase in V/Eu ratio from 1.0 to 1.5 and decreased with further increase in V/Eu molar ratio. The highest acetone conversion was obtained on catalyst $V_{1.5}Eu_1O_x$. The acetone conversion reached 98.0% under both UV and visible light. The result of Fig. 6 shows that the $VEuO_x$ composite catalysts are as active as P25 under UV light. Under visible light, it shows much higher photoactivity than P25, $EuVO_4$, or V_2O_5. Obviously, loading of V_2O_5 to $EuVO_4$ formulated a series of active photodegradation catalysts.

In the photodegradation of acetone, the typical degradation products are CO_2, CO, acetol, and H_2O. As an example, for the photodegradation of acetone over $V_{1.5}Eu_1O_x$, the selectivities to CO_2, CO, and acetol are 39.3%, 60.5%, and 0.2%, respectively (Table 2). It means that the $V_{1.5}Eu_1O_x$ catalyst was not able to oxidize acetone completely. There are significant amount of CO and acetol left as partial oxidation products which are still viewed as pollutants. Loading a small amount of noble metal (such as Pt, Au, Ag, and Ru) to photocatalyst is a practical way to achieve the complete oxidation of organic pollutants [15,16,30,31]. The loaded metal could change the distribution of the electrons in a photocatalyst and form the Schottky barriers at each metal–semiconductor contact region, which leads to charge separation. Among the noble metals, it is reported that Pt is the most effective component [31]. Hence, we loaded the $V_{1.5}Eu_1O_x$ catalyst with a small amount of Pt (0.1 wt.%). Table 2 shows the testing results under visible light irradiation. The 0.1 wt.% $Pt/V_{1.5}Eu_1O_x$ catalyst shows higher conversion of acetone than catalyst $V_{1.5}Eu_1O_x$, and only CO_2 and H_2O were detected in the degradation products. It was also proven to be efficient for the oxidation of methanol, ethanol, 2-propanol, and benzene (Table 2). Obviously, the Pt doped $V_{1.5}Eu_1O_x$ catalyst is a better photodegradation catalyst in terms of both activity and complete oxidation.

The stability of $VEuO_x$ composite catalysts was evaluated by continuous reaction. Fig. 7 shows the life-testing results of $V_{1.5}Eu_1O_x$ and 0.1 wt.% $Pt/V_{1.5}Eu_1O_x$ catalysts under visible light. Both catalysts were stable within 24 h of continuous reaction. An average acetone conversion of 99.4% was obtained over 0.1 wt.% $Pt/V_{1.5}Eu_1O_x$ catalyst. For $V_{1.5}Eu_1O_x$ catalyst, the average acetone conversion reached 98%. The results of Fig. 7 indicate that the $V_{1.5}Eu_1O_x$ catalyst is promising for practical application for air purification because of its high activity and stability.

3.3. Discussion

The composite photocatalysts have attracted increasing attention for their enhanced performance. Yet present explanations are

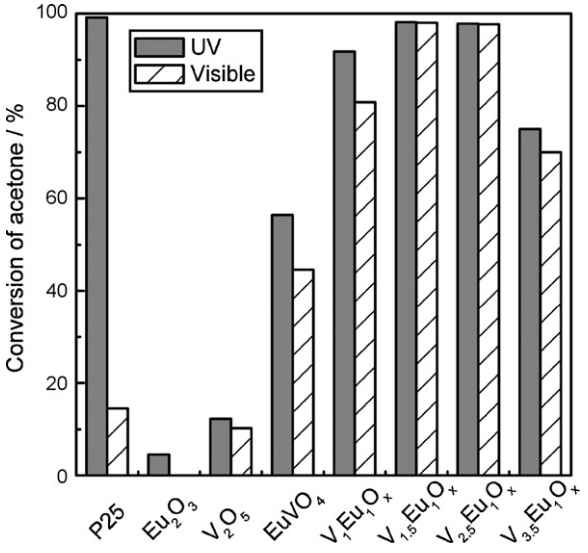

Fig. 6. Acetone photodegradation over $VEuO_x$ composite catalysts.

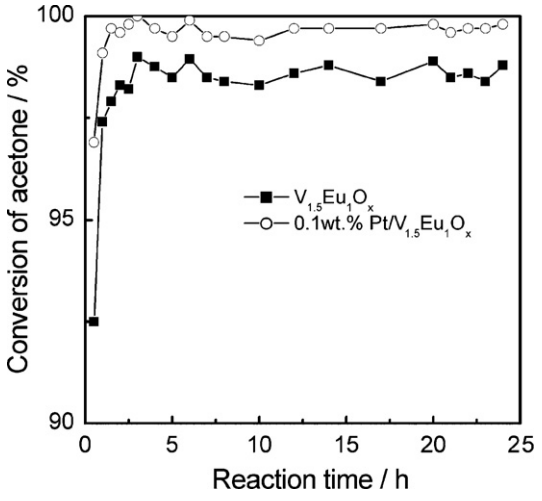

Fig. 7. Effect of reaction time on the performance of $V_{1.5}Eu_1O_x$ and 0.1 wt.% $Pt/V_{1.5}Eu_1O_x$ catalysts.

Table 3
Absolute electronegativity, estimated band gap, energy levels of calculated conduction band edge, and valence band at the point of zero charge for V_2O_5 and $EuVO_4$.

Semiconductor oxides	Absolute electronegativity (X)	Estimated energy band gap, E_g (eV)	Calculated conduction band edge (eV)	Calculated valence band edge (eV)
V_2O_5	6.4817	2.08	0.94	3.02
$EuVO_4$	5.8312	2.24	0.21	2.45

still far from clarifying it. Some researchers attribute the increased activity to the adsorption ability for the organic compounds, which are often related to the specific surface area [32,33]. In the present case of $VEuO_x$ composites, a correlation consistency between specific surface area and photoactivity was not observed. The $V_1Eu_1O_x$ (47 m^2/g) and $V_{2.5}Eu_1O_x$ (20 m^2/g) catalyst showed lower acetone conversion than $V_{1.5}Eu_1O_x$ (25 m^2/g) catalyst under both UV and visible light. Hence, we think the specific surface area is not a major factor to influence the photoactivity of $VEuO_x$ catalysts. The most important factor might be the composition of the catalysts.

Different measures of characterization have revealed that only the V_2O_5 and $EuVO_4$ phases exist in the $VEuO_x$ composite catalysts. V_2O_5 is inactive because of the rapid recombination of electron–hole pairs [34]. But when it was coupled with $EuVO_4$ the photocatalytic activity was greatly improved. It shows the typical phenomenon of the coupled photocatalyst. So, it is plausible that the stronger photoactivity of the $VEuO_x$ composite catalysts results from the coupling effect between V_2O_5 and $EuVO_4$.

The coupling effect is involved in retarding the recombination of the photogenerated charges, which is one of the limiting factors in photocatalytic phenomena. Many researchers have noted the particularity of the photocatalytic properties of composite systems, consisting of two semiconductors in contact, and attributed the improvement in activity to the enhanced charge separation [25–27,34–36]. The coupling of two semiconductors possessing different redox energy levels for their corresponding conduction and valence bands allows to achieve more efficient charge separation, increase the lifetime of the charge carriers and thus enhance the efficiency of the interfacial charge transfer to adsorbed substrates. In the current case, we think the charge migration also occurs between $EuVO_4$ and V_2O_5 semiconductors. In order to prove the above suggestion, the band energy potentials of the V_2O_5 and $EuVO_4$ semiconductors are needed. There are three methods to determine the band edge positions: experiments based on photoelectrochemical techniques, calculation according to first principle, and predicting theoretically from the absolute (or Mulliken) electronegativity [37–39]. The first one is not always easy to handle, and the second one cannot obtain the absolute energy of band edges with respect to vacuum and always has large discrepancies between calculated and measured values. The third one is a simple approach with reasonable results for many oxide photocatalysts [38,39]. The conduction band edge of a semiconductor at the point of zero charge (pH_{zpc}) can be predicted by $E^0_{CB} = X - E_c - (1/2)E_g$. Where X is the absolute electronegativity of the semiconductor, expressed as the geometric mean of the absolute electronegativity of the constituent atoms, which is defined as the arithmetic mean of the atomic electron affinity and the first ionization energy; E_c is the energy of free electrons on the hydrogen scale (~4.5 eV); and E_g is the band gap of the semiconductor. Table 3 shows the predicted band edge positions of V_2O_5 and $EuVO_4$ by the above equation. In fact, these values are slightly more anodic than the measured value but this does not affect the comparison of their relative positions. As shown in Table 3, the conduction band of $EuVO_4$ is more cathodic than the conduction band of V_2O_5, while the valence band of V_2O_5 is more positive than the corresponding band of $EuVO_4$. It means that their valence and conduction bands are suitably disposed. As shown in Fig. 8, the conduction band of V_2O_5 will act as a sink for the photogenerated electrons while hole transfer occurs

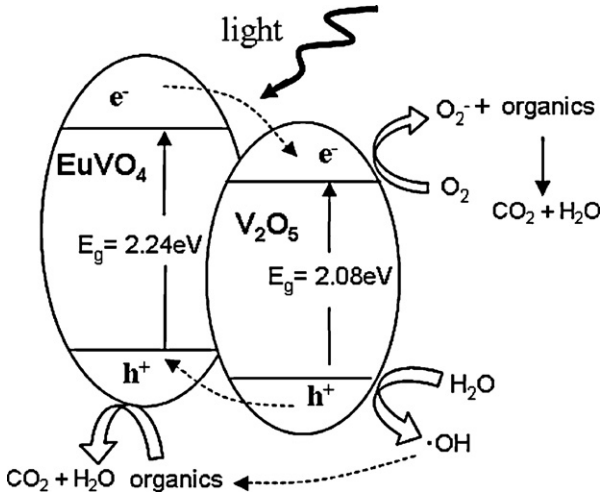

Fig. 8. Photo-excitation and simultaneous charge transfer processes for the couple $EuVO_4$–V_2O_5 semiconductor.

from the valence band of V_2O_5 to that of $EuVO_4$. This simultaneous charge transfer could increase the space charge separation, limit their recombination and thus increase the photo-oxidation efficiency.

The above analysis could also be proved by the photoluminescence (PL) spectra of the photocatalysts, which are useful to disclose the migration, transfer, and recombination processes of the photogenerated electron–hole pairs in the semiconductor [40]. Fig. 9 shows the PL spectra of $EuVO_4$ and $V_{1.5}Eu_1O_x$ catalysts. The PL spectrum of $EuVO_4$ shows three strong emissions at 451, 592, and 617 nm, indicating that the electrons and holes recombine rapidly [41,42]. However, over $V_{1.5}Eu_1O_x$ catalyst, the peaks intensity is greatly decreased. It suggests that the loading with V_2O_5 retarded the electron–hole pair recombination. This is consistent with the analysis of the coupling effect, as discussed above.

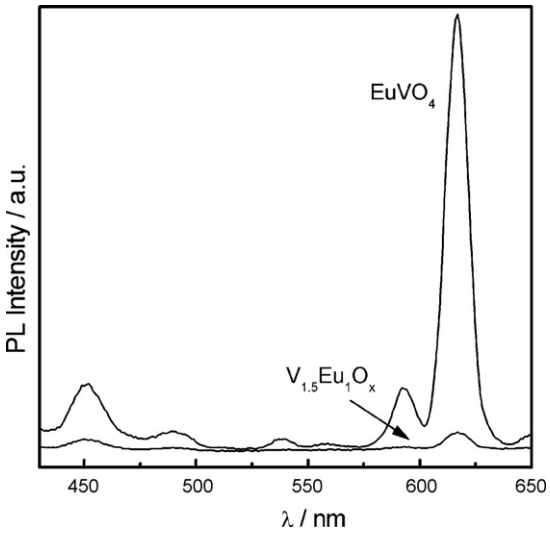

Fig. 9. PL spectra of $EuVO_4$ and $V_{1.5}Eu_1O_x$ composite.

4. Conclusions

$VEuO_x$ composite photocatalyst which could be described as V_2O_5 doped $EuVO_4$ catalyst has been synthesized from the aqueous of solutions of $Eu(NO_3)_3$ and NH_4VO_3. $V_{1.5}Eu_1O_x$ catalyst was found to be the best one. 98% conversion of acetone was obtained under visible light. The mechanism has been discussed by the calculated energy band positions and PL spectra. The enhanced activity is attributed to the coupling effect between $EuVO_4$ and V_2O_5, which retards the recombination of photogenerated hole–electron pairs. The composite photocatalyst is promising for air purification application for its good activity and stability. By loading a small amount of Pt the performance of catalyst can be further improved.

Acknowledgements

This work was supported by grants from the 973 Program (2007CB815301 and 2006CB932904), the National Science Foundation of China (20333070, 20673118, and 20871114), the Science Foundation of CAS (KJCX2-YW-M05) and of Zhejiang Education Department (Y200909374), the Research Initiation Funds for the Doctor of Zhejiang Normal University (ZC304008169) and the Technology Funds of Jinhua (2009-1-169).

References

[1] A. Fujishima, K. Honda, Nature 238 (1972) 37.
[2] D.S. Bhatkhande, V.G. Pangarkar, A.A. Beenackers, J. Chem. Technol. Biotechnol. 77 (2001) 101.
[3] J. Zhao, X.D. Yang, Build. Environ. 38 (2003) 645.
[4] A. Fujishima, T.N. Rao, D.A. Tryk, J. Photochem. Photobiol. C: Photochem. Rev. 1 (2000) 1.
[5] W. Choi, A. Termin, M.R. Hoffmann, J. Phys. Chem. 98 (1994) 13669.
[6] H. Yamashita, M. Harada, J. Misaka, M. Takeuchi, K. Ikeue, M. Anpo, J. Photochem. Photobiol. A 148 (2002) 257.
[7] R. Ashi, T. Morikawa, T. Ohwaki, K. Aoki, Y. Taga, Science 293 (2001) 269.
[8] S. Sakthivel, H. Kisch, Angew. Chem., Int. Ed. 42 (2003) 4908.
[9] J.W. Tang, Z.G. Zou, J.H. Ye, Angew. Chem., Int. Ed. 43 (2004) 4463.
[10] A. Kudo, H. Kato, I. Tsuji, Chem. Lett. 33 (2004) 1534.
[11] A. Kudo, K. Ueda, H. Kato, I. Mikami, Catal. Lett. 53 (1998) 229.
[12] S. Tokunaga, H. Kato, A. Kudo, Chem. Mater. 13 (2001) 4624.
[13] B. Muktha, G. Madras, T.N. Guru Row, J. Photochem. Photobiol. A 187 (2007) 177.
[14] H.G. Kim, D.W. Hwang, J.S. Lee, J. Am. Chem. Soc. 126 (2004) 8912.
[15] T. Ishihara, N.S. Baik, N. Ono, H. Nishiguchi, Y. Takita, J. Photochem. Photobiol. A 167 (2004) 149.
[16] T. Ohno, S. Izumi, K. Fujihara, M. Matsumura, J. Photochem. Photobiol. A 129 (1999) 143.
[17] M.C. Long, W.M. Cai, J. Cai, B.X. Zhou, X.Y. Chai, Y.H. Wu, J. Phys. Chem. B 110 (2006) 20211.
[18] K. Teramura, K. Maeda, T. Saito, T. Takata, N. Saito, Y. Inoue, K. Domen, J. Phys. Chem. B 109 (2005) 21915.
[19] S. Kohtani, J. Hiro, N. Yamamoto, A. Kudo, K. Tokumura, R. Nakagaki, Catal. Commun. 6 (2005) 185.
[20] S. Kohtani, M. Tomohiro, K. Tokumura, R. Nakagaki, Appl. Catal. B 58 (2005) 265.
[21] Z.M. Fang, Q. Hong, Z.H. Zhou, S.J. Dai, W.Z. Weng, H.L. Wan, Catal. Lett. 61 (1999) 39.
[22] Z.M. Fang, J. Zou, W.Z. Weng, H.L. Wan, Stud. Surf. Sci. Catal. 119 (1998) 629.
[23] G. Chen, R.G. Haire, J.R. Peterson, M.M. Abraham, J. Phys. Chem. Solids 55 (1994) 313.
[24] G.F. Wang, W.P. Qin, D.S. Zhang, L.L. Wang, G.D. Wei, P.F. Zhu, R. Kim, J. Phys. Chem. C 112 (2008) 17042.
[25] S.T. Marin, C.L. Morrison, M.R. Hoffmann, J. Phys. Chem. 98 (1994) 13695.
[26] Y.M. He, T.L. Sheng, J.S. Chen, R.B. Fu, R.M. Hu, X.T. Wu, Catal. Commun. 10 (2009) 1354.
[27] Y.M. He, Y. Wu, H. Guo, T.L. Sheng, X.T. Wu, J. Hazard. Mater. 169 (2009) 855.
[28] T. Ono, Y. Tanaka, T. Takeuchi, K. Yamamoto, J. Mol. Catal. A: Chem. 159 (2000) 293.
[29] M. Prasad, A.K. Pandit, T.H. Ansari, R.A. Singh, B. M/Wanklyn, Phys. Lett. A 138 (1989) 61.
[30] T.A. Egerton, J.A. Mattinson, J. Photochem. Photobiol. A: Chem. 194 (2008) 283.
[31] F. Chen, J. Wang, J.Q. Xu, X.P. Zhou, Appl. Catal. A: Gen. 348 (2008) 54.
[32] M.E. Simonsen, H. Jensen, Z.S. Li, E.G. Søgaard, J. Photochem. Photobiol. A 200 (2008) 192.
[33] H.L. Yu, K.L. Zhang, C. Rossi, J. Photochem. Photobiol. A 188 (2007) 65.
[34] F. Chen, J. Wang, T.H. Wu, X.P. Zhou, Catal. Commun. 9 (2008) 1698.
[35] V. Keller, F. Garin, Catal. Commun. 4 (2003) 377.
[36] J. Papp, S. Soled, K. Dwight, A. Wold, Chem. Mater. 6 (1994) 496.
[37] Y.I. Kim, S.J. Atherton, E.S. Brigham, T.E. Mallouk, J. Phys. Chem. 97 (1993) 11802.
[38] M.A. Butler, D.S. Ginley, J. Electrochem. Soc. 125 (1978) 228.
[39] Y. Xu, M.A.A. Schoonen, Am. Mineral. 85 (2000) 543.
[40] J.W. Tang, Z.G. Zou, J.H. Ye, J. Phys. Chem. B 107 (2003) 14265.
[41] F.B. Li, X.Z. Li, Appl. Catal. A: Gen. 228 (2002) 15.
[42] J.Y. Shi, J. Chen, Z.C. Feng, T. Chen, Y.X. Lian, X.L. Wang, C. Li, J. Phys. Chem. C 111 (2007) 693.